Critical behavior of megabase-size DNA toward the transition into a compact state.

AUTHOR(S):

Yoshikawa, Yuko; Suzuki, Yuki; Yamada, Kozo; Fukuda, Wakao; Yoshikawa, Kenichi; Takeyasu, Kunio; Imanaka, Tadayuki

CITATION:

Yoshikawa, Yuko ...[et al]. Critical behavior of megabase-size DNA toward the transition into a compact state.. The Journal of chemical physics 2011, 135(22): 225101.

ISSUE DATE:

2011-12-14

URL:

http://hdl.handle.net/2433/152375

Critical behavior of megabase-size DNA toward the transition into a compact state

Yuko Yoshikawa, Yuki Suzuki, Kozo Yamada, Wakao Fukuda, Kenichi Yoshikawa et al.

Citation: J. Chem. Phys. **135**, 225101 (2011); doi: 10.1063/1.3666845
View online: http://dx.doi.org/10.1063/1.3666845
View Table of Contents: http://jcp.aip.org/resource/1/JCPSA6/v135/i22
Published by the American Institute of Physics.

THE JOURNAL OF CHEMICAL PHYSICS **135**, 225101 (2011)

Critical behavior of megabase-size DNA toward the transition into a compact state

Yuko Yoshikawa,[1,2] Yuki Suzuki,[3] Kozo Yamada,[1] Wakao Fukuda,[1,2] Kenichi Yoshikawa,[4,a)] Kunio Takeyasu,[3] and Tadayuki Imanaka[1,2]
[1]*Department of Biotechnology, College of Life Sciences, Ritsumeikan University, Kusatsu 525-8577, Japan*
[2]*CREST, JST, Kawaguchi 332-0012, Japan*
[3]*Laboratory of Plasma Membrane and Nuclear Signaling, Graduate School of Biostudies, Kyoto University, Kyoto 606-8502, Japan*
[4]*Department of Physics, Graduate School of Science, Kyoto University, Kyoto 606-8501, Japan*

(Received 22 August 2011; accepted 17 November 2011; published online 8 December 2011)

We studied the changes in the higher-order structure of a megabase-size DNA (S120-1 DNA) under different spermidine (SPD) concentrations through single-molecule observations using fluorescence microscopy (FM) and atomic force microscopy (AFM). We examined the difference between the folding transitions in S120-1 DNA and sub-megabase-size DNA, T4 DNA (166 kbp). From FM observations, it is found that S120-1 DNA exhibits intra-chain segregation as the intermediate state of transition, in contrast to the all-or-none nature of the transition on T4 DNA. Large S120-1 DNA exhibits a folding transition at lower concentrations of SPD than T4 DNA. AFM observations showed that DNA segments become aligned in parallel on a two-dimensional surface as the SPD concentration increases and that highly intense parallel alignment is achieved just before the compaction. S120-1 DNA requires one-tenth the SPD concentration as that required by T4 DNA to achieve the same degree of parallel ordering. We theoretically discuss the cause of the parallel ordering near the transition into a fully compact state on a two-dimensional surface, and argue that such parallel ordering disappears in bulk solution. © *2011 American Institute of Physics*. [doi:10.1063/1.3666845]

I. INTRODUCTION

In living cells, large DNA molecules up to several centimeters long are highly compacted and show different levels of ordered structures.[1] The manner of DNA packaging is expected to play a very important role in the regulation of gene expression.[2–5] *In vitro* condensation/compaction of DNA has long been of interest as a potential model for DNA packaging *in vivo*.[6] Over the past several decades, numerous *in vitro* studies have been performed to understand the physicochemical properties of condensed DNA.[1,7–22] *In vitro* condensation and compaction of DNA can be achieved by various chemical agents.[14,16] Polyamines,[9,23–27] metal cations,[28–32] neutral polymers,[8,33,34] polypeptides,[34] and basic proteins[35–37] have all been found to be very efficient condensing agents. Electron microscopy studies have shown that condensed DNA assumes toroid, spheroid, and rod-like structures.[20] However, most of these studies were performed on short DNAs such as plasmid DNA of several kbp without a clear distinction between single-molecule packing and multi-molecule aggregation.[38]

Over the past decade, we have investigated the changes in the higher-order structure of a large DNA molecule through a single-molecule observation using FM.[39–47] To visualize individual DNA molecules, we used T4 phage DNA (166 kbp) as a model large DNA, and its size is on the order of a chromatin loop domain (∼100 kbp).[48] We found that giant DNA molecules undergo an on/off transition from an expanded coil state to a compact state accompanied by a difference in density on the order of 10^4–10^5 upon the addition of various condensing agents including polyamines,[40,41] basic proteins,[49] and neutral polymers,[50] while short DNA fragments behave like rigid rods and cannot undergo such a folding transition.[4,38,51]

Here, we extended our investigation to a megabase-size genomic DNA (S120-1 DNA) that was successfully extracted from *Rhodoligotrophos appendicifer* (strain 120-1^T = JCM 16873^T = ATCC BAA 2115^T).[52] Strain 120-1^T was isolated from a freshwater lake in Antarctica and is characterized by slow growth and low rates of metabolism associated with its oligotrophic environment. Both of these features may enable us to successfully isolate large genomic DNA fragments of near-megabase size. The original genome of strain 120-1^T is 5.66 Mbp with a circular structure and its G+C content is 61.1 mol%. To characterize the compaction process of S120-1 DNA at the single-molecule level, we used a combination of fluorescence microscopy (FM) and atomic force microscopy (AFM). The term "megabase-size DNA" as used herein refers to a linear duplex DNA fragment with the typical size of ∼800 kbp, as evaluated through the direct measurement by FM. We used spermidine (SPD), a trivalent polyamine, as a condensing agent to induce the folding transition. It is known that polyamines such as spermidine and spermine exist at submillimolar to millimolar concentrations and strongly influence the packaging process of DNAs in bacteria[53,54] and

a)Author to whom correspondence should be addressed. Electronic mail: yoshikaw@scphys.kyoto-u.ac.jp.

viruses.[54] In this study, we compared the changes in the higher-order structure of S120-1 DNA to those of T4 DNA (166 kbp) in a quantitative manner.

II. EXPERIMENTAL METHODS

A. Materials

T4 phage DNA (166 kbp, contour length 57 μm) was purchased from Nippon Gene (Toyama, Japan). A fluorescent cyanine dye, YOYO-1, (quinolinium,1,1′-[1,3-propanediyl-bis[(dimethyliminio)-3,1-propanediyl]] bis[4-[(3-methyl-2(3H)-benzoxazolylidene)methyl]]-tetraiodide) was purchased from Molecular Probes Inc. (Eugene, OR, USA). The antioxidant 2-mercaptoethanol (2-ME) was purchased from Wako Pure Chemical Industries (Osaka, Japan). Other chemicals were of analytical grade and were obtained from various commercial sources.

B. Preparation of genomic DNA from *R. appendicifer* strain 120-1^T

R. appendicifer strain 120-1^T, a Gram-negative, non-spore-forming, non-motile, irregularly circular, aerobic bacterium, was collected from the surface water of Naga-ike, a freshwater lake, in the Skarvsnes, Antarctica, by the summer party of the 46th Japanese Antarctic Research Expedition in 2004–2005. Strain 120-1^T grows between 5 and 35 °C, with an optimum temperature of 30 °C. The OD_{660} reaches a maximum value of about 1.2 after incubation for about 120 h. Other features of strain 120-1^T were described in detail in our recent study.[52]

S120-1 DNA was extracted by the following procedures. Strain 120-1^T was cultivated in 0.25 × Luria-Bertani medium (2.50 g/l of tryptone, 1.25 g/l of yeast extract, 5.0 g/l of NaCl, pH 7) at 30 °C for 5 days with gentle shaking. To extract genomic DNA from the strain, 5 ml of cell suspension was centrifuged at 6000 rpm for 3 min. After the supernatant was removed, the cells were re-suspended in 400 μl TE buffer (10 mM Tris-HCl, 1 mM EDTA, pH 8.5). Next, cells were treated with 4 mg/ml of lysozyme to weaken the cell walls at 37 °C for 30 min. After incubation, cells were lysed by treatment with 40 μl of 10% SDS solution, and a phenol/chloroform/isoamyl alcohol mixture (25:24:1) was then added to the tube to remove proteins. After centrifugation at 15 000 rpm for 10 min, the sample was mixed with 1/10 volume of 3 M sodium acetate and 100% ethanol, stored at −20 °C for 20 min, and then centrifuged at 12 000 rpm, 4 °C for 10 min. Further purification was performed with cold 70% ethanol. After the sample was centrifuged for 10 min at 12 000 rpm, 4 °C, the pellet was dried for 2 min using a vacuum centrifuge and re-suspended in 50 μl TE buffer containing 100 μg/ml RNase to remove residual RNA. The purity of extracted genomic DNA was determined spectrophotometrically at an absorbance ratio of 260/280 nm (A260/A280) using a NanoDrop ND-1000 spectrophotometer (Thermo Fisher Scientific, Inc., Waltham, MA, USA). The A260/A280 value of 1.7–1.9 indicated that the extracted DNA was of high quality.

C. Direct observation of the change in the conformation of DNA in bulk solution and on a glass surface by FM

All of the FM observations were performed under aqueous environment. T4 phage DNA or S120-1 genomic DNA was dissolved in 10 mM Tris-HCl buffer and 4% (v/v) 2-mercaptoethanol at pH 7.6 in the absence or presence of SPD. Measurements were conducted at a low DNA concentration (0.3 μM in nucleotide units). SPD concentrations were varied from 0.01 mM to 1 mM. To visualize individual DNA molecules by FM, the cyanine dye YOYO-1 (0.05 μM) was added to the DNA solution. YOYO-1 is known to bind to double-stranded DNA through base-pair intercalation and has been reported to show a strong increase in fluorescence upon binding to DNA.[55] Images of extended single DNA molecules on glass surfaces were obtained as follows. Microscope glasses were pre-treated with 0.05% (v/v) poly-(L-lysine) solution, washed repeatedly with distilled water, and dried in air. A droplet (15 μL) of a sample solution was adsorbed on a cationically modified glass slide. After the slide was allowed to stand at room temperature for 1 or 2 min, we prepared the sample by inducing weak convective flow with a pipette to obtain extended DNAs, and the slide was then covered with a slip glass. All of images were obtained using an inverted fluorescence microscope (Axiovert 135 TV; Carl Zeiss, Oberkochen, Germany) equipped with 100× or 40× oil-immersion objective lens and a highly sensitive EBCCD camera (Hamamatsu Photonics, Shizuoka, Japan), which made it possible to record images on DVD. The video images were analyzed with an image-analysis software, Cosmos32, (Library; Tokyo, Japan).

D. AFM observation of single DNA molecules

For AFM imaging using Multi Mode AFM (Digital Instruments, Santa Barbara, CA, USA), DNA samples were dropped onto a freshly cleaved mica surface. After incubation for 10 min at room temperature, the mica was rinsed with water and dried under nitrogen gas. The DNA concentration and buffer condition were the same as in the FM observations. All imaging was performed in air using the cantilever tapping mode. The cantilever (OMCL-AC160TS-W2, Olympus) was 129 μm long and had a spring constant of 33–62 N/m. The scanning frequency was 1–3 Hz, and images were captured using the height mode in a 512 × 512 pixel format. The obtained images were plane-fitted and flattened by the computer program supplied with the imaging module before analysis.

III. RESULTS

A. FM observations of the higher-order structure of single DNA molecules

Representative FM images of S120-1 genomic DNA fixed on a glass surface are shown in Figs. 1(a)–1(d), where observed S120-1 DNA molecules (500–900 kbp) are much larger than T4 DNA (166 kbp) (Fig. 1(e)). AFM made it possible to visualize the highly extended fiber structure of S120-1 DNA in the presence of a low concentration of SPD

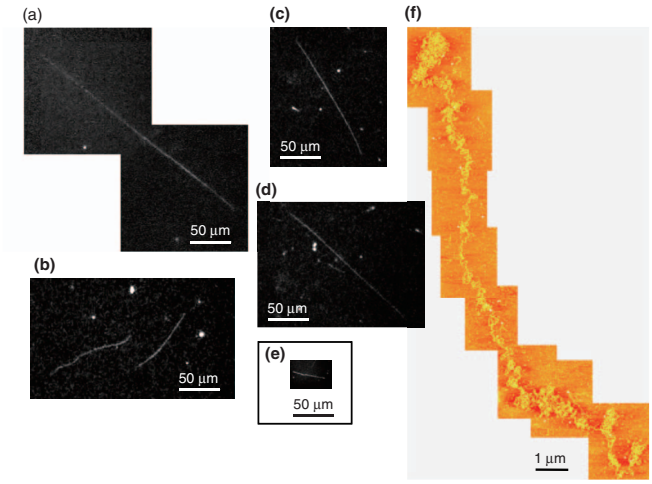

FIG. 1. FM images of S120-1 DNA (a)–(d) and T4 DNA molecules (e) on a glass surface in aqueous environment, and an AFM image of S120-1 DNA on a mica surface in dry state (f). (a)–(e) DNAs are extended by inducing weak convective flow with a pipette in 10 mM Tris-HCl buffer at pH 7.6 and fixed on a glass surface, (f) DNA sample is gently adsorbed on a mica surface in 10 mM Tris-HCl buffer with 0.01 mM SPD at pH 7.6, and then rinsed with water and dried before the measurement.

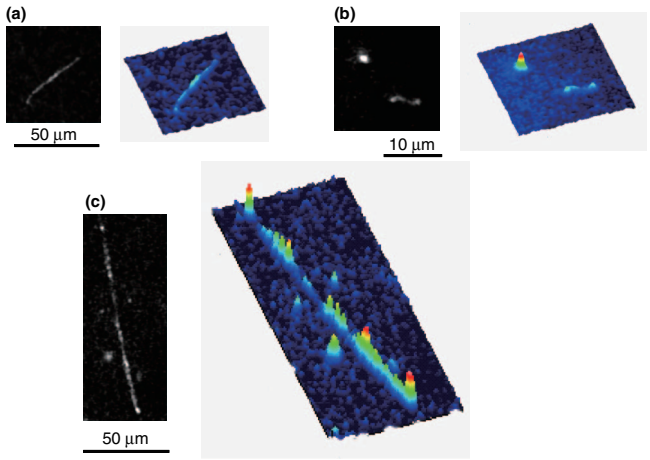

FIG. 3. FM images of T4 DNA (a) and (b) and S120-1 DNA (c) in the presence of 0.1 mM SPD and corresponding quasi-three-dimensional profile of the fluorescence intensity. (a) and (c) On a glass surface in aqueous environment and (b) in bulk solution. In (b), the coexistence of coil and globule DNAs is observed, where only 0.5%–1% of T4 DNA molecules exhibit a compacted globule state.

(0.01 mM) (Fig. 1(f)). Figure 2 shows FM images of individual DNA molecules thermally fluctuating in solution. A quasi-3D profile of fluorescence intensity is shown at the bottom of each fluorescence image. In the buffer solution, both T4 and S120-1 DNA molecules exist as an elongated coil conformation with long-axis lengths of 5 and 20 μm, respectively (Figs. 2(a)–2(d)). In the presence of 0.1 mM SPD, T4 DNA molecules still show a coil conformation (Fig. 2(b)), similar

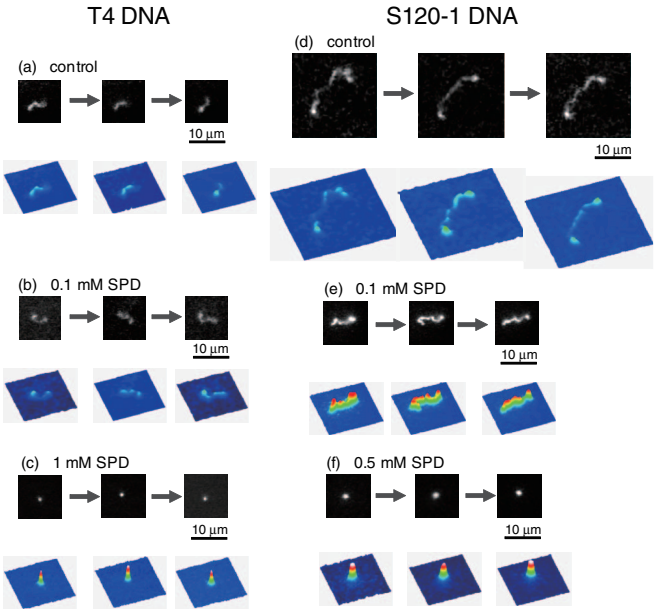

FIG. 2. Real-time monitoring of a single DNA molecule in bulk solution with various concentrations of SPD and corresponding quasi-three-dimensional profile of the fluorescence intensity. Total observation time is 1 s for all of the successive pictures. In (a), (b), (d), and (e), Brownian fluctuations are seen for both translational and intra-chain motions. In (c) and (f), the images of the compact state are situated at the center of each frame by shifting the position of the objects because of their significant translational Brownian motion; on the order of 5–10 μm for 1 s.

to that in buffer solution (Fig. 2(a)), whereas S120-1 DNA molecules show a change in conformation to a shrunken structure (Fig. 2(e)). At 0.5 mM SPD, S120-1 DNA becomes a bright optical spot, which reflects the appearance of a compact state (Fig. 2(f)), while most of the T4 DNA molecules remain in the coil state at 0.5 mM SPD (data not shown). At 1 mM SPD, T4 DNA shows a compact state. (Fig. 2(c)).

More detailed information on the shrunken structure was obtained when the DNA molecules were spread on a glass surface (Figs. 3(a) and 3(c)). With the addition of 0.1 mM SPD, S120-1 DNA shows a beaded structure in which compact and elongated parts coexist in a single DNA molecule (Figs. 3(c)). On the other hand, most of the T4 DNA molecules exhibit a coiled structure without highly compacted parts along a DNA chain in the presence of 0.1 mM SPD (Fig. 3(a)); only 0.5%–1% of T4 DNA molecules exhibits a compact globule state in the presence of 0.1 mM SPD. Figure 3(b) shows the coexistence of coil and globule T4 DNAs in bulk solution with 0.1 mM SPD. These results suggest that more SPD is required to compact T4 DNA than is needed for larger S120-1 DNA.

B. AFM observation of the higher-order structure of single DNA molecules

To determine the detailed critical behavior before DNA compaction on a sub-micro scale, AFM observations were performed for both T4 and S120-1 DNA. The AFM images in Fig. 4 have a high enough resolution to clearly distinguish the degree of compaction in T4 and S120-1 DNA in response to various concentrations of SPD. With the addition of 0.1 mM SPD, a looping structure consisting of essentially straight chains with parallel alignment appeared in S120-1 DNA (Fig. 4(g)), whereas T4 DNA maintained a random orientation (Fig. 4(b)). These results are in good agreement with the FM observations (Figs. 2 and 3); S120-1 DNA exhibits a folding transition at much lower concentrations of SPD than T4 DNA. A further increase in the SPD concentration above

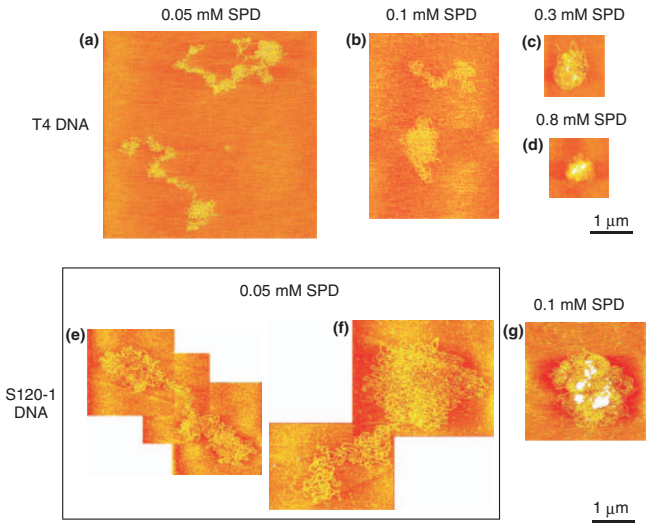

FIG. 4. AFM images of DNA molecules at various concentrations of SPD in dry state. All of the specimens are gently adsorbed on the mica surface without shear stress.

0.3 mM also induces parallel alignment in the T4 DNA chain (Figs. 4(c) and 4(d)). The apparent degree of shrinkage in the structure of T4 DNA in 0.8 mM SPD is similar to that of S120-1 DNA in 0.1 mM SPD. Figure 5 shows the AFM images of megabase-size DNA and short fragments derived from S120-1 DNA in the presence of the same concentration of SPD (0.1 mM). It is clear that short fragments remain in a dispersed state (Fig. 5(b)) under the condition that causes the large-scale parallel alignment for the megabase-size DNA (Fig. 5(a)).

IV. DISCUSSION

The present results demonstrate that S120-1 DNA is more sensitive to the SPD concentration than T4 DNA. The degree of compaction observed by FM (Figs. 2 and 3) corresponds well with that observed by AFM (Fig. 4). Further inspection of the AFM images in Fig. 4 suggests that the parallel alignment between DNA segments is enhanced as the SPD concentration increases. It is also noted that locally aligned segments constitute circles with different curvature, suggesting the parallel ordering is not due to the lattice structure of mica surface. Similar effects on the appearance of parallel ordering have been described in previous reports.[56–58] However, the degree of parallel ordering has not yet been fully analyzed quantitatively at the single-molecule level.

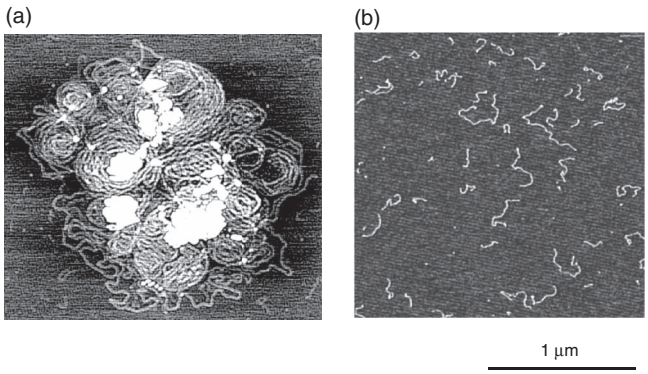

FIG. 5. AFM images of S120-1 DNA in the presence of 0.1 mM SPD. (a) Megabase-size DNA (an enlarged image of Fig. 4(g)), and (b) short fragments produced by mechanical agitation (pipetting and shaking) of S120-1 DNA.

A. Evaluation of the degree of parallel alignment

To evaluate the degree of parallel alignment observed by AFM in a quantitative manner, we analyzed the change in conformation by considering the difference in the angles between nearby segments. The actual procedure used for the analysis is depicted in Fig. 6. We arbitrarily chose a straight line on an AFM microgram and determined the angle difference between neighboring DNA segments:

$$\Delta\theta_i = \theta_{i+1} - \theta_i. \tag{1}$$

We adapted $\cos 2\Delta\theta_i$ as a measure of the degree of parallel orientation between the neighboring DNA segments in two dimensions. The order parameter S was then calculated

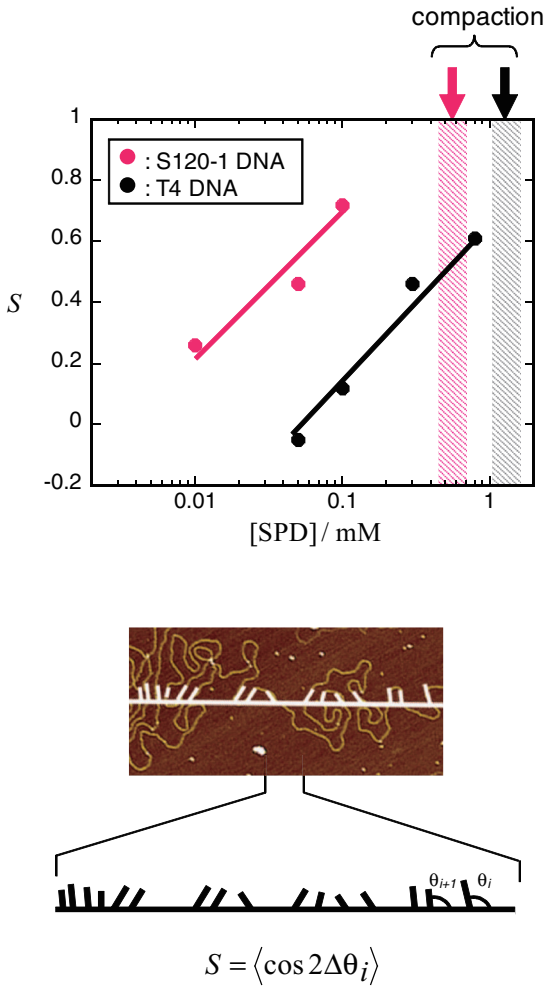

FIG. 6. Dependence of the degree of parallel ordering, $S = \langle \cos 2\Delta\theta_i \rangle$, on the logarithm of the SPD concentration (top graph). The illustration shows how we evaluated the degree of ordering from the AFM image. In the actual procedure, the S value is averaged for the data set of cross-sectional lines with different angles. Detail of the procedure to calculate S value is given in the text.

by taking the ensemble average of about 40–50 data points for each DNA molecules using the equation:

$$S = \langle \cos 2\Delta\theta_i \rangle . \quad (2)$$

In Eq. (2), the ensemble average was deduced from the angle difference $\Delta\theta_i$ along multiple straight lines with different orientations on the AFM image. Figure 6 shows the change in the order parameter S at different SPD concentrations for both T4 and S120-1 DNA, where we adapted the logarithms of the sperimidine concentration, log[SPD]. Segment orientation is clearly enhanced with an increase in the SPD concentration, and S120-1 DNA is more sensitive than T4 DNA, consistent with the difference in the folding transition between these two DNAs. S120-1 DNA requires only one-tenth the SPD concentration to show the same degree of parallel ordering as T4 DNA. In Fig. 6, it is noted that the degree of the parallel ordering S is linearly correlated with log[SPD]. It has been demonstrated that the manner of the folding transition of single DNA by a multivalent cation, such as SPD, is properly interpreted in term of the free energy change including the activity of the cation.[41] In other words, the free energy change is described as a linear function of the logarithm of the multivalent cation concentration. It may be, therefore, reasonably to expect the linearity between the degree of ordering as a measure of the DNA conformation and log[SPD].

B. Enhanced parallel ordering near compaction on a 2D surface

We discuss here why segment alignment is enhanced on a 2D surface with an increase in the SPD concentration just before the appearance of the fully compact state. Under the framework of the counterion condensation theory for a rod-like polyelectrolyte chain,[59,60] negative phosphate groups along a double-helical DNA chain are shielded by up to ~90% in response to the addition of SPD (3+) in aqueous solution, in other words, 10% of negative charge still survive. Therefore, the enhancement of parallel alignment just before the compaction as shown in Fig. 4 is attributed to the self-avoiding volume interaction between DNA segments due to the surviving negative charge, under the shrinking effect in the segregated state. Here, it is noted that the counterion condensation theory applies to an isolated rod-like polyelectrolyte chain, but not to a fully collapsed polyelectrolyte. Actually, it has been well established that DNA is almost fully neutralized after the compaction.[61] FM observations as shown in Fig. 2 also indicate that SPD causes the shrinkage of DNA because of the formation of bridges or crossings on the long DNA chain. Such shrinkage may promote parallel ordering on a two-dimensional surface as described in the following mechanism.

We consider a DNA with a contour length $L = N\lambda$, where N is the number of segments and λ is the Kuhn length, or twice the persistence length.[62] We consider the effective area, A, occupied by a DNA molecule as $A = \pi R^2$, where R is the average radius on a 2D surface and may be almost equal with the radius of gyration. If individual segments assume an orientation in a random manner, we can estimate the area occupied by a single segment, a, as $a \approx \pi\lambda^2/4$. Thus, the total occupied area in a random coiled DNA becomes $Na \approx \pi N\lambda^2/4$. The segment length, or Kuhn length, of double-strand DNA is ~100 nm or ~300 bp. We may estimate the total occupied area as $Na \approx 2\ \mu\text{m}^2$ for a DNA of 0.1 Mbp and $Na \approx 20\ \mu\text{m}^2$ for a DNA of 1 Mbp. On the other hand, the radius of gyration of a DNA with random coil conformation on 2D is give as $R_g \approx \lambda N^{3/4}$ (Ref. 32), suggesting the total area of the coil DNA to be $A = \pi R_g^2 \approx \pi\lambda^2 N^{3/2}$, $A \approx 200\ \mu\text{m}^2$, and $A \approx 6000\ \mu\text{m}^2$ for the DNAs of 0.1 and 1 Mbp, respectively. Obviously, the condition of $A \gg Na$ is fulfilled for the random coil DNA, indicating that parallel alignment is never generated as actually depicted in the AFM observations (see Fig. 1(f)). In contrast, when $A < \pi N\lambda^2$, as in the state just before the folding transition, DNA segments assume a parallel orientation due to the self-avoiding volume effect between the segments. Here, we may expect the promotion of the shrinking of DNA on 2D surface because of the generation of plural number of crossings between segments just before the compaction. The cooperation between the repulsive interaction and the shrinking effect on 2D, thus, causes the parallel alignment.

C. Difference between 2D surface and 3D solution

As the next, we discuss the differences in the DNA conformations between the bulk (3D) and the surface (2D). Because of the difficulty to deduce the actual conformation of DNA in bulk solution by use of current experimental tools, here we will interpret on the basis of theoretical considerations. We adapt the situation for a DNA on a 2D surface where the average difference on the orientation between the neighboring segments is $\langle\theta_2\rangle$. For simplicity, hereafter $\langle\theta_2\rangle$ is expressed as θ_2 .The self-avoiding volume by a single segment is estimated to be $a \approx \lambda^2 \sin\theta_2$, and the total occupied area by a whole DNA molecule is now $A = \pi R^2 \approx Na$. Thus, we obtain the following relationship for the 2D conformation.

$$\sin\theta_2 \approx \pi R^2/N\lambda^2. \quad (3)$$

As the next, we assume a DNA in bulk solution, where the difference of the orientation between the neighboring segments is $\langle\theta_3\rangle$; for simplicity hereafter we use the symbol of θ_3. The volume occupied by a segment is then deduced to be $v \approx \pi\lambda^3 \sin^2\theta_3$. By adapting the similar argument as in the 2D case, we obtain the following relationship:

$$\sin^2\theta_3 \approx 4R^3/3N\lambda^3. \quad (4)$$

When the effective radius R is the same between 2D and 3D, we obtain the relation between θ_2 and θ_3, from Eqs. (3) and (4).

$$\sin\theta_3 \approx \frac{2N^{1/4}}{3^{1/2}\pi^{3/4}}(\sin\theta_2)^{3/4}. \quad (5)$$

To examine the above relationship on the observations in the present study, we consider the case of $\sin\theta_2 = 1/2$, i.e., $\theta_2 = \pi/6$ or $\cos 2\theta_2 = 1/2$, which corresponds to a relatively weak parallel ordering on 2D. After simple calculation, we obtain $\sin\theta_3 \approx 1.3$ when $N = 330$ (0.1 megabase-size DNA), and $\sin\theta_3 \approx 2.2$ when $N = 3300$ (1 megabase-size DNA). Violation of the mathematical restriction of $|\sin\theta_3|$

≤ 1, thus, means the absence of parallel alignment in the bulk solution (3D).

Summarizing the above discussion, it has become clear that the appearance of parallel ordering is the characteristics generated on 2D for the DNA molecules just before the compaction, whereas it should be absent in 3D solution. In relation to the mechanism of the parallel ordering of DNA, it is to be noted that self-avoiding effect is the main driving force to cause the isotropic-nematic phase transition in a liquid crystal.[63]

D. Difference in the higher-order structural change between S120-1 DNA and T4 DNA

To explain the higher sensitivity of S120-1 DNA with regard to both compaction and parallel alignment, we can consider the difference in stiffness. The G+C contents of S120-1 DNA and T4 DNA are 61% and 34%, respectively, suggesting that the persistence length of S120-1 DNA is much greater than that of T4 DNA. Since the compact state of DNA is characterized by almost perfect parallel ordering among the segments, we can expect that the compact state with a greater G+C content will be more stable. This expectation corresponds well with the previous observation that the region with a higher G+C content acts as a nucleation center in the kinetics of the folding transition.[64] In addition, longer DNA may prefer a compact state due to the higher probability of the crossing of segments along a single DNA molecule. Similar phenomena have been reported in observations on DNA molecules smaller than several tens of kbp.[28,65] That is, longer DNA molecules tend to "condense" at lower concentrations of condensing agents, which corresponds to our observations shown in Fig. 5.

E. Intra- and inter-chain segregation

The FM observations in Fig. 3 reveal that, near the transition region between the elongated and compact states, S120-1 DNA exhibits "intra-chain segregation," whereas T4 DNA tends to show "inter-chain segregation," as depicted in the schematic illustrations (Fig. 7). Thus, for S120-1 DNA, a tightly compact part and an elongated part coexist along a single DNA molecule (Fig. 7(a)), which is attributable to the bimodal free-energy profile with minima of the elongated and compact states. On the other hand, for T4 DNA, the transition between the two states is always an all-or-none type over individual DNA molecules (Fig. 7(b)), which also reflects the bimodal free-energy profile. The difference between S120-1 and T4 DNA molecules is thus considered to be the difference in the correlation length/size at the folding transition.[66] The general trend of segregation along a giant DNA is considered to be associated with the mechanism of selective activation/inhibition of certain specific genes along long genomic DNA in living cells.

In summary, we gain insight into important intrinsic properties of megabase-size DNA. The appearance of the phase-segregated state in megabase-size DNA is markedly different from the all-or-none characteristics on the folding transition in a single sub-megabase-size DNA. In addition, it is shown that just before the full compaction giant DNA molecules tend to exhibit highly parallel ordering when DNA is situated on a 2D surface, whereas in bulk, there should exist no parallel alignment. In the segregated state of megabase-size DNA, the uncondensed part of the chain tends to exhibit a highly parallel orientation when DNA is interacting with a 2D surface, which may correspond to a biomembrane in living cells.[67] The plausible effect of the higher G+C content in S120-1 DNA on the higher sensitivity to the multivalent cation, SPD, would be unveiled in a near future through the comparative studies with other megabase-size DNA from different biological sources. Further studies on the folding transition of megabase-size and still larger DNAs from various genome sources may help to reveal the biological significance of this change in the higher-order structure.

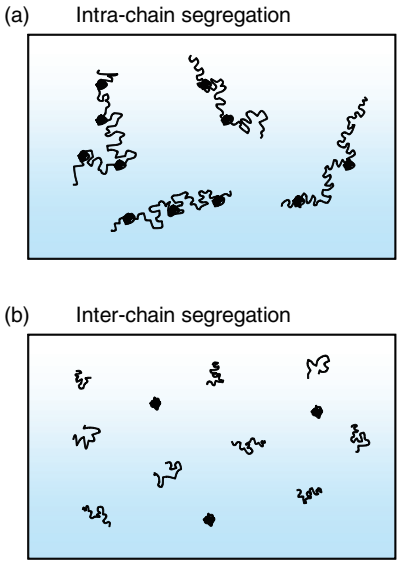

FIG. 7. Schematic illustrations of different intermediate states between coil and compact conformations of DNA.

ACKNOWLEDGMENTS

This work was supported in part by Grants-in-Aid for Scientific Research from the Ministry of Education, Culture, Sports, Science and Technology of Japan (18GS0421) and from the Japan Society for the Promotion of Science (22510123, 23240044, and 23657068). Y. S. is a recipient of the JSPS Research Fellow.

APPENDIX: INTRA-CHAIN SEGREGATION ON GIANT DNA

We will simply explain why intra-chain segregated state appears for the megabase-sized DNA,[66] while inter-chain segregation is observed for smaller DNA, as schematically shown in Fig. 6. We consider a long DNA molecule with the number of segments, N, where one segment corresponds to the Kuhn length, ~100 nm or ~300 bp. Taking the free energy of a elongated coil state as the reference, we obtain the

free-energy on a compact state as

$$\Delta F \approx -aN + bN^{2/3} + c\frac{Q^2}{R}. \quad \text{(A1)}$$

In Eq. (A1), *a, b, c* are positive constants, and the first and second terms are volume and surface energy, respectively. The last term indicates the contribution from the Coulomb repulsion due to the surviving negative charge inside the compact state. Under the assumption of nearly spherical morphology on the compact state, we may assume that $R^{-1} \sim N^{-1/3}$ and $Q^2 \sim N^2$. We thus obtain the following relationship.

$$\Delta F \approx -aN + bN^{2/3} + c'N^{5/3}. \quad \text{(A2)}$$

This equation implies that the free energy of the compact state becomes positive above a threshold value N_c, indicating the breakdown of the mean-field argument as in the above equations. In other words, when the DNA size is above N_c, $N > N_c$, segregated state along a single molecule becomes the most stable state, in which the compact part in the segregated state is composed with the number of segments smaller than N_c. On the other hand, when $N < N_c$, individual DNA molecules undergoes all-or-none transition between coil and compact states. Detailed theoretical considerations on the stability of the phase-segregated conformation on a single DNA molecule including the effect of counter ion were described in our previous studies.[44,66]

[1] Y. Fang and J. H. Hoh, Nucleic Acids Res. **26**, 588 (1998).
[2] I. Baeza, P. Gariglio, L. M. Rangel, P. Chavez, L. Cervantes, C. Arguello, C. Wong, and C. Montanez, Biochemistry **26**, 6387 (1987).
[3] J. Pelta, D. Durand, J. Doucet, and F. Livolant, Biophys. J. **71**, 48 (1996).
[4] K. Tsumoto, F. Luckel, and K. Yoshikawa, Biophys. Chem. **106**, 23 (2003).
[5] A. Yamada, K. Kubo, T. Nakai, K. Yoshikawa, and K. Tsumoto, Appl. Phys. Lett. **86**, (2005).
[6] C. C. Conwell, I. D. Vilfan, and N. V. Hud, Proc. Natl. Acad. Sci. U.S.A. **100**, 9296 (2003).
[7] M. Haynes, R. A. Garrett, and W. B. Gratzer, Biochemistry **9**, 4410 (1970).
[8] Y. M. Evdokimov, A. L. Platonov, A. S. Tikhonenko, and Y. M. Varshavsky, FEBS Lett. **23**, 180 (1972).
[9] L. C. Gosule and J. A. Schellman, Nature (London) **259**, 333 (1976).
[10] S. A. Allison, J. C. Herr, and J. M. Schurr, Biopolymers **20**, 469 (1981).
[11] C. B. Post and B. H. Zimm, Biopolymers **21**, 2123 (1982).
[12] V. A. Bloomfield, Biopolymers **31**, 1471 (1991).
[13] N. V. Hud, M. J. Allen, K. H. Downing, J. Lee, and R. Balhorn, Biochem. Biophys. Res. Commun. **193**, 1347 (1993).
[14] V. A. Bloomfield, Curr. Opin. Struct. Biol. **6**, 334 (1996).
[15] K. Yoshikawa and Y. Matsuzawa, J. Am. Chem. Soc. **118**, 929 (1996).
[16] V. A. Bloomfield, Biopolymers **44**(3), 269 (1997).
[17] O. Lambert, L. Letellier, W. M. Gelbart, and J. L. Rigaud, Proc. Natl. Acad. Sci. U.S.A. **97**, 7248 (2000).
[18] N. V. Hud and K. H. Downing, Proc. Natl. Acad. Sci. U.S.A. **98**, 14925 (2001).
[19] I. D. Vilfan, C. C. Conwell, and N. V. Hud, J. Biol. Chem. **279**(19), 20088 (2004).
[20] N. V. Hud and I. D. Vilfan, Annu. Rev. Biophys. Biomol. Struct. **34**, 295 (2005).
[21] I. D. Vilfan, C. C. Conwell, T. Sarkar, and N. V. Hud, Biochemistry **45**, 8174 (2006).
[22] B. A. Todd and D. C. Rau, Nucleic Acids Res. **36**, 501 (2008).
[23] D. K. Chattoraj, L. C. Gosule, and J. A. Schellman, J. Mol. Biol. **121**, 327 (1978).
[24] W. Wilson and V. A. Bloomfield, Biochemistry **18**, 2192 (1979).
[25] K. A. Marx and T. C. Reynolds, Biochim. Biophys. Acta **741**, 279 (1983).
[26] D. Porschke, Biochemistry **23**(21), 4821 (1984).
[27] D. Jary and J. L. Sikorav, Biochemistry **38**, 3223 (1999).
[28] J. Widom and R. L. Baldwin, Biopolymers **22**, 1595 (1983).
[29] J. A. Schellman and N. Parthasarathy, J. Mol. Biol. **175**, 313 (1984).
[30] D. Gersanovski, P. Colson, C. Houssier, and E. Fredericq, Biochim. Biophys. Acta **824**, 313 (1985).
[31] H. A. Tajmir-Riahi, R. Ahmad, and M. Naoui, J. Biomol. Struct. Dyn. **10**, 865 (1993).
[32] C. L. Ma and V. A. Bloomfield, Biophys. J. **67**, 1678 (1994).
[33] L. S. Lerman, Cold Spring Harb. Symp. Quant. Biol. **38**, 59 (1974).
[34] U. K. Laemmli, Proc. Natl. Acad. Sci. U.S.A. **72**, 4288 (1975).
[35] D. E. Olins and A. L. Olins, J. Mol. Biol. **57**, 437 (1971).
[36] D. J. Clark and J. O. Thomas, J. Mol. Biol. **187**, 569 (1986).
[37] M. Garciaramirez and J. A. Subirana, Biopolymers **34**, 285 (1994).
[38] K. Yoshikawa and Y. Yoshikawa, in *Pharmaceutical Perspectives of Nucleic Acid-Based Therapy*, edited by R. I. Mahato and S. W. Kim (Taylor & Francis, London, 2002), p. 136.
[39] Y. Matsuzawa and K. Yoshikawa, Nucleosides Nucleotides **13**, 1415 (1994).
[40] Y. Yoshikawa and K. Yoshikawa, FEBS Lett. **361**, 277 (1995).
[41] M. Takahashi, K. Yoshikawa, V. V. Vasilevskaya, and A. R. Khokhlov, J. Phys. Chem. B **101**, 9396 (1997).
[42] S. M. Melnikov, V. G. Sergeyev, and K. Yoshikawa, J. Am. Chem. Soc. **117**, 2401 (1995).
[43] K. Yoshikawa, S. Kidoaki, M. Takahashi, V. V. Vasilevskaya, and A. R. Khokhlov, Ber. Bunsenges. Phys. Chem. **100**, 876 (1996).
[44] K. Yoshikawa, Y. Yoshikawa, Y. Koyama, and T. Kanbe, J. Am. Chem. Soc. **119**, 6473 (1997).
[45] Y. Yoshikawa, Y. S. Velichko, Y. Ichiba, and K. Yoshikawa, Eur. J. Biochem. **268**, 2593 (2001).
[46] Y. Katsuda, Y. Yoshikawa, T. Sato, Y. Saito, M. Chikuma, M. Suzuki, and K. Yoshikawa, Chem. Phys. Lett. **473**, 155 (2009).
[47] N. Kida, Y. Katsuda, Y. Yoshikawa, S. Komeda, T. Sato, Y. Saito, M. Chikuma, M. Suzuki, T. Imanaka, and K. Yoshikawa, J. Biol. Inorg. Chem. **15**, 701 (2010).
[48] H. H. Heng, J. B. Stevens, G. Liu, S. W. Bremer, and C. J. Ye, Cell Chromosome **3**, 1 (2004).
[49] N. Makita, Y. Yoshikawa, Y. Takenaka, T. Sakaue, M. Suzuki, C. Watanabe, T. Kanai, T. Kanbe, T. Imanaka, and K. Yoshikawa, J. Phys. Chem. B **115**, 4453 (2011).
[50] K. Minagawa, Y. Matsuzawa, K. Yoshikawa, A. R. Khokhlov, and M. Doi, Biopolymers **34**, 555 (1994).
[51] H. Oana, K. Tsumoto, Y. Yoshikawa, and K. Yoshikawa, FEBS Lett. **530**, 143 (2002).
[52] W. Fukuda, K. Yamada, Y. Miyoshi, H. Okuno, H. Atomi, and T. Imanaka, "*Rhodoligotrophos appendicifer* gen. nov., sp. nov., a bacterium with projections isolated from a lake in Skarvsnes, Antartica," Int. J. Syst. Evol. Microbiol. (in press).
[53] I. Flink and D. E. Pettijohn, Nature (London) **253**, 62 (1975).
[54] Z. Lin, C. Wang, X. Z. Feng, M. Z. Liu, J. W. Li, and C. L. Bai, Nucleic Acids Res. **26**, 3228 (1998).
[55] H. S. Rye, S. Yue, D. E. Wemmer, M. A. Quesada, R. P. Haugland, R. A. Mathies, and A. N. Glazer, Nucleic Acids Res. **20**, 2803 (1992).
[56] Y. Fang and J. H. Hoh, J. Am. Chem. Soc. **120**, 8903 (1998).
[57] Y. T. A. Chim, J. K. W. Lam, Y. Ma, S. P. Armes, A. L. Lewis, C. J. Roberts, S. Stolnik, S. J. B. Tendler, and M. C. Davies, Langmuir **21**, 3591 (2005).
[58] K. Besteman, K. van Eijk, I. D. Vilfan, U. Ziese, and S. G. Lemay, Biopolymers **87**, 141 (2007).
[59] F. Oosawa, Biopolymers **9**, 677 (1970).
[60] G. S. Manning, Q. Rev. Biophys. **11**, 179 (1978).
[61] Y. Yamasaki, Y. Teramoto, and K. Yoshikawa, Biophys. J. **80**, 2823 (2001).
[62] N. Yoshinaga, K. Yoshikawa, and S. Kidoaki, J. Chem. Phys. **116**, 9926 (2002).
[63] P. G. De Gennes and J. Prost, *The Physics of Liquid Crystals*, *2nd edition*. (Oxford University Press, Oxford, 1993).
[64] Y. Matsuzawa, Y. Yonezawa, and K. Yoshikawa, Biochem. Biophys. Res. Commun. **225**, 796 (1996).
[65] E. Raspaud, M. Olvera de la Cruz, J. L. Sikorav, and F. Livolant, Biophys. J. **74**, 381 (1998).
[66] T. Iwaki and K. Yoshikawa, Europhys. Lett. **68**, 113 (2004).
[67] H. G. Hansma, Annu. Rev. Phys. Chem. **52**, 71 (2001).